Decrease in glucose transporter 1 levels and translocation of glucose transporter 3 in the dentate gyrus of C57BL/6 mice and gerbils with aging

Kwon Young Lee[1], Dae Young Yoo[2], Hyo Young Jung[2], Loktam Baek[3], Hangyul Lee[3], Hyun Jung Kwon[4], Jin Young Chung[5], Seok Hoon Kang[6], Dae Won Kim[4], In Koo Hwang[2], Jung Hoon Choi[1,*]

[1]Department of Anatomy, College of Veterinary Medicine and Institute of Veterinary Science, Kangwon National University, Chuncheon, Korea
[2]Department of Anatomy and Cell Biology, College of Veterinary Medicine, and Research Institute for Veterinary Science, Seoul National University, Seoul, Korea
[3]Undergraduate School, College of Veterinary Medicine, Seoul National University, Seoul, Korea
[4]Department of Biochemistry and Molecular Biology, Research Institute of Oral Sciences, College of Dentistry, Gangneung-Wonju National University, Gangneung, Korea
[5]Department of Veterinary Internal Medicine and Geriatrics, College of Veterinary Medicine and Institute of Veterinary Science, Kangwon National University, Chuncheon, Korea
[6]Department of Medical Education, Kangwon National University School of Medicine, Chuncheon, Korea

In the present study, we compared the cell-specific expression and changes protein levels in the glucose transporters (GLUTs) 1 and 3, the major GLUTs in the mouse and gerbil brains using immuno-histochemistry and Western blot analysis. In both mouse and gerbils, GLUT1 immunoreactivity was mainly found in the blood vessels in the dentate gyrus, while GLUT3 immunoreactivity was detected in the subgranular zone and the molecular layer of the dentate gyrus. GLUT1-immunoreactivity in blood vessels and GLUT1 protein levels were significantly decreased with age in the mice and gerbils, respectively. In addition, few GLUT3-immunoreactive cells were found in the subgranular zone in aged mice and gerbils, but GLUT3-immunoreactivity was abundantly found in the polymorphic layer of dentate gyrus in mice and gerbils with a dot-like pattern. Based on the double immunofluorescence study, GLUT3-immunoreactive structures in gerbils were localized in the glial fibrillary acidic protein-immunoreactive astrocytes in the dentate gyrus. Western blot analysis showed that GLUT3 expression in the hippocampal homogenates was slightly, although not significantly, decreased with age in mice and gerbils, respectively. These results indicate that the reduction in GLUT1 in the blood vessels of dentate gyrus and GLUT3 in the subgranular zone of dentate gyrus may be associated with the decrease in uptake of glucose into brain and neuroblasts in the dentate gyrus. In addition, the expression of GLUT3 in the astrocytes in polymorphic layer of dentate gyrus may be associated with metabolic changes in glucose in aged hippocampus.

Keywords: Glucose transporter, aging, dentate gyrus, neuroblasts, blood vessels, astrocytes

Glucose is the primary source of energy for every cell in the body and the brain utilizes 20% of the glucose in the body for maintaining its function, although the brain consists of only about 2% of the total body weight [1].

For the entry of glucose into the central nervous system, glucose transporters 1 and 3 (GLUT1 and GLUT3) are essential [2-4]. GLUT1 is present in endothelial cells and astrocytes, which are consisted of blood-brain barrier [5-

*Corresponding author: Jung Hoon Choi, Department of Anatomy, College of Veterinary Medicine and Institute of Veterinary Science, Kangwon National University, Chuncheon 24341, Korea
Tel: +82-33-250-8682; Fax: +82-33-244-2367; E-mail: jhchoi@kangwon.ac.kr

7], whereas GLUT3 is mainly found in neurons [3,4]. More than 50% deficiency of GLUT1 can lead to structural abnormalities in the mouse brain [8] and the zebrafish brain [9]. In contrast, heterozygous GLUT3 mutant mice show normal development in the body and brain size, but display cognitive abnormalities without changes in the normal exploratory, sniffing, and rearing behaviors and motor ability [10].

Aging is one of the most important and universal contributors to the etiologies of metabolic decline and related diseases. Several lines of evidence indicate the reduction in brain glucose utilization with aging [11,12]. However, physical exercise for 1-3 weeks increases the mRNA levels of GLUT1 and GLUT3 in the cerebral cortex [13]. In addition, ischemic tolerance transiently increases GLUT3 expression in the brain [14], and the administration of GLUT3 siRNA reduces the effects of preconditioning on ischemic tolerance [15]. Morphological studies have showed that GLUT3 immunoreactivity is found in the mossy fibers of the CA3 region, stratum radiatum of the CA1 region, and the granule cell layer and hilar region of the dentate gyrus of the mouse hippocampus [16] and rat [17]. In our previous study, we showed that GLUT3 immunoreactivity is found in the subgranular zone of the dentate gyrus and GLUT3 is co-localized with doublecortin (DCX)-immunoreactive neuroblasts in the dentate gyrus of the postnatal mouse brain [18]. In this regard, GLUT3 can also modulate hippocampal neurogenesis in the subgranular zone of the dentate gyrus.

However, morphological findings related to GLUT1 and GLUT3 immunoreactivity in the hippocampus are limited. Hence, in the present study we investigated changes in the GLUT1 and GLUT3 immunoreactivity in the dentate gyrus, and colocalization of GLUT3-immuno-reactive cells and DCX-immunoreactive neuroblasts in the dentate gyrus.

Materials and Methods

Experimental animals

Adult (4-month-old), mid-aged (18-month-old), and aged (24-month-old) male C57BL/6J mice and gerbils were purchased from Japan SLC, Inc. (Hamamatsu, Shizuoka, Japan). Eighteen- and twenty-four-month-old mice and gerbils were chosen as the aged group, as an age of 18 and 24 months is equivalent to the human age of 56 and 69 years, respectively [19]. The animals were placed in a mouse cage (5 mice per cage) and a rat cage (3 gerbils per cage) in conventional condition with adequate temperature (22ºC) and humidity (60%) controls, a 12-hour light/12-hour dark cycle with *ad libitum* access to food and water. The handling and care of the animals conformed to guidelines compliant with current international laws and policies (NIH Guide for the Care and Use of Laboratory Animals, NIH Publication No. 85-23, 1985, revised 1996). Ethical approval was obtained from the Institutional Animal Care and Use Committee of Kangwon National University (Chuncheon, Gangwon, Republic of Korea) for all animal procedures in the present study (no. KW-160802-2). All experiments were conducted with an effort to minimize the number of animals used and the suffering caused by the procedures employed in the study.

Tissue processing

Mice (*n*=5 per group) and gerbils (*n*=5 per group) at postnatal month 4 (PM4), PM18, and PM24 were anesthetized with 1 g/kg urethane (Sigma-Aldrich, St. Louis, MO) and were transcardially perfused with 0.1 M phosphate-buffered saline (PBS; pH 7.4), followed by perfusion with 4% paraformaldehyde in 0.1 M PBS (pH 7.4). The brains were dissected and fixed in the same fixative for 12 h before performing cryoprotection by means of overnight storage in 30% sucrose. Serial coronal brain sections (thickness, 30 μm) were obtained using a cryostat (Leica, Wetzlar, Germany) and collected into six-well plates containing 0.1 M PBS (pH 7.4). To ensure that the immunohistochemical data were comparable between groups, sections were carefully processed in parallel. Tissue sections located 90-μm apart were selected from sections spanning an area between 1.46 and 2.46 mm posterior to the bregma, as defined by the mouse atlas [20] and between 1.40 to 1.80 mm posterior to the bregma, as described by gerbil brain atlas [21].

Immunohistochemistry

Five sections from the tissue sections located 90 μm apart were sequentially incubated with 0.3% hydrogen peroxide (H_2O_2) in PBS (pH 7.4) for 30 minutes and with 10% normal goat serum in 0.05 M PBS for 30 minutes as described by a previous study [22]. The sections were then incubated with rabbit anti-GLUT1 (1:200; Abcam, Cambridge, UK) or rabbit anti-GLUT3 (1:50; SantaCruz Biotechnology, Santa Cruz, CA, USA) antibodies overnight at 25ºC. The sections were then

incubated with biotinylated goat anti-rabbit IgG and then with a streptavidin-peroxidase complex (1:200; Vector Laboratories Inc., Burlingame, CA, USA). Immuno-staining was visualized by reaction with 3,3'-diamino-benzidine tetrachlodride (DAB) in 0.1 M Tris-HCl buffer (pH 7.2). The sections were dehydrated and mounted on gelatin-coated slides in Canada balsam (Kanto Chemical, Tokyo, Japan). In order to establish the specificity of the GLUT1 and GLUT3 antibodies, the procedure included the omission of the GLUT1 and GLUT3 antibodies, goat anti-rabbit IgG, and the substitution of normal goat serum for the primary antibody. But, we could not find any positive signals in this test.

Double immunofluorescence

To confirm the colocalization of GLUT3 and glial fibrillary acidic protein (GFAP) in the aged gerbil brain, the sections were processed by double immuno-fluorescence staining under the same conditions. Double immunofluorescence staining for rabbit anti-GLUT3 (1:20)/mouse anti-GFAP (diluted 1:25; SantaCruz Biotechnology) was performed. The sections were incubated in the mixture of antisera overnight at 25ºC. After washing with PBS thrice for 10 min each, the slices were then incubated in a mixture of both FITC-conjugated donkey anti-rabbit IgG (1:600; Jackson ImmunoResearch, West Grove, PA) and Cy3-conjugated donkey anti-mouse IgG (1:600; Jackson Immuno Research) for 2 h at 25ºC. Immunoreactivity was observed under the confocal microscope (LSM510 META NLO, Carl Zeiss, Göttingen, Germany).

Western blot analysis

To quantify changes in GLUT1 and GLUT3 levels within the dentate gyrus, gerbils (n=6 in each group) at PM4, PM18, and PM24 were euthanized and their brains were removed. Tissues were dissected for use in Western blot analysis. In brief, 500-μm-thick sections were obtained using a vibratome (Leica Microsystems, GmbH, Germany), and the area consisting of the dentate gyrus was sub-dissected using a surgical blade. The dentate gyrus-containing vials was homogenized in 50 mM PBS (pH 7.4) containing 0.1 mM ethylene glycol-bis(2-amino-ethylether)-N,N,N,N-tetraacetic acid (pH 8.0); 0.2% Nonidet P-40; 10 mM ethylenediaminetetraacetic acid (pH 8.0); 15 mM sodium pyrophosphate; 100 mM β-glycerophosphate; 50 mM NaF; 150 mM NaCl; 2 mM sodium orthovanadate; 1 mM phenylmethylsulfonyl fluoride;

and 1 mM dithiothreitol (DTT). After centrifugation, the protein level in the supernatant was determined using a Micro BCA protein assay kit according to the manufacturer's instructions (Pierce Chemical, Rockford, IL). Aliquots containing 20 μg of total protein were denatured by boiling them in loading buffer containing 150 mM Tris (pH 6.8), 3 mM 1,4-dithiothreitol (DTT), 6% sodium dodecyl sulfate, 0.3% bromophenol blue, and 30% glycerol. Each aliquot was loaded onto a polyacrylamide gel. After electrophoresis, the proteins were transferred onto nitrocellulose membranes (Pall Crop, East Hills, NY), which were then blocked in 5% non-fat dry milk in PBS/0.1% Tween 20 for 45 minutes, prior to incubation with a rabbit anti-GLUT1 antibody (1:500; Abcam) or a rabbit anti-GLUT3 antibody (1:100; SantaCruz Biotechnology). Then, the membranes were incubated with peroxidase-conjugated anti-rabbit IgG (1:400; Vector Laboratories Inc.) and visualization was conducted by an enhanced luminol-based chemilumines-cence kit (Pierce Chemical). The blots were scanned, and densitometry was performed using the Scion Image software (Scion Corp., Frederick, MD). The blots were then stripped and reprobed with an antibody against β-actin as an internal loading control. The data were normalized to the β-actin level in each lane.

Statistical analysis

The data are presented as mean±SEM. The differences between group means were statistically analyzed using the Student's *t*-test performed in the GraphPad Prism 5.01 software (GraphPad Software, Inc., La Jolla, CA). The results with $P<0.05$ were considered statistically significant.

Results

Age-related changes in GLUT1 immunoreactivity and protein levels in the dentate gyrus

GLUT1 immunoreactivity was mainly found in the blood vessels in the dentate gyrus of mice and gerbils at PM4, PM18, and PM24. In the PM4 group, GLUT1 immunoreactivity was abundantly found in the molecular, granule cell, and polymorphic layers of the dentate gyrus in mice and gerbils. In addition, strongly GLUT1 immunoreactive structures were also found in the subgranular zone of the dentate gyrus (Figure 1). In mice and gerbils at PM18, GLUT1 immunoreactive blood vessels were found in the dentate gyrus, and GLUT1
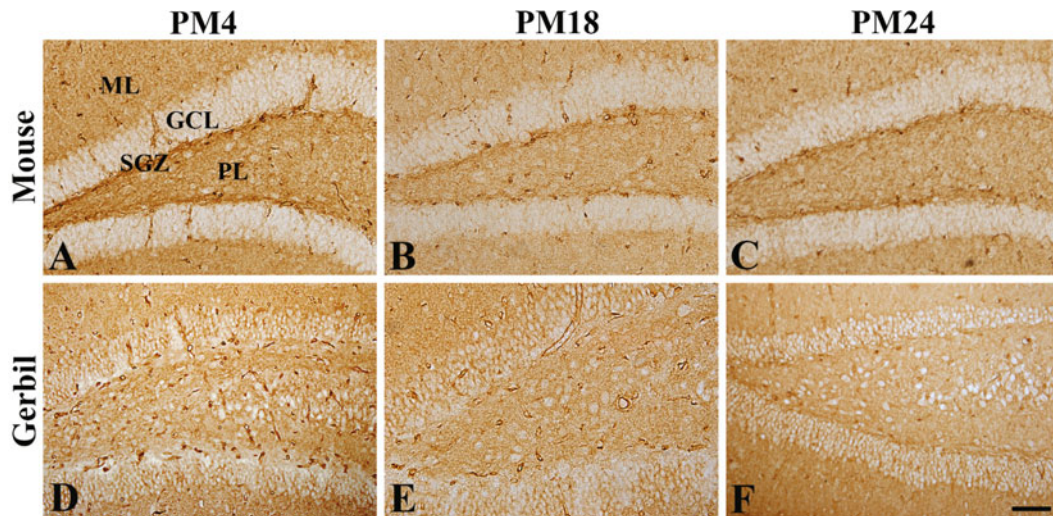
Figure 1. Immunohistochemistry for GLUT1 in the dentate gyrus of mice (A, B, and C) and gerbils (D, E, and F) at postnatal month 4 (PM4, A and D), PM18 (B and E), and PM24 (C and F). GLUT1 immunoreactivity is found in the blood vessel-like structures in the hippocampus. Note that GLUT1-immunoreactive structures are decreased with age in both rodents. Scale bar=50 μm. ML, molecular layer; GCL, granule cell layer; PL, polymorphic layer; SGZ, subgranular zone.
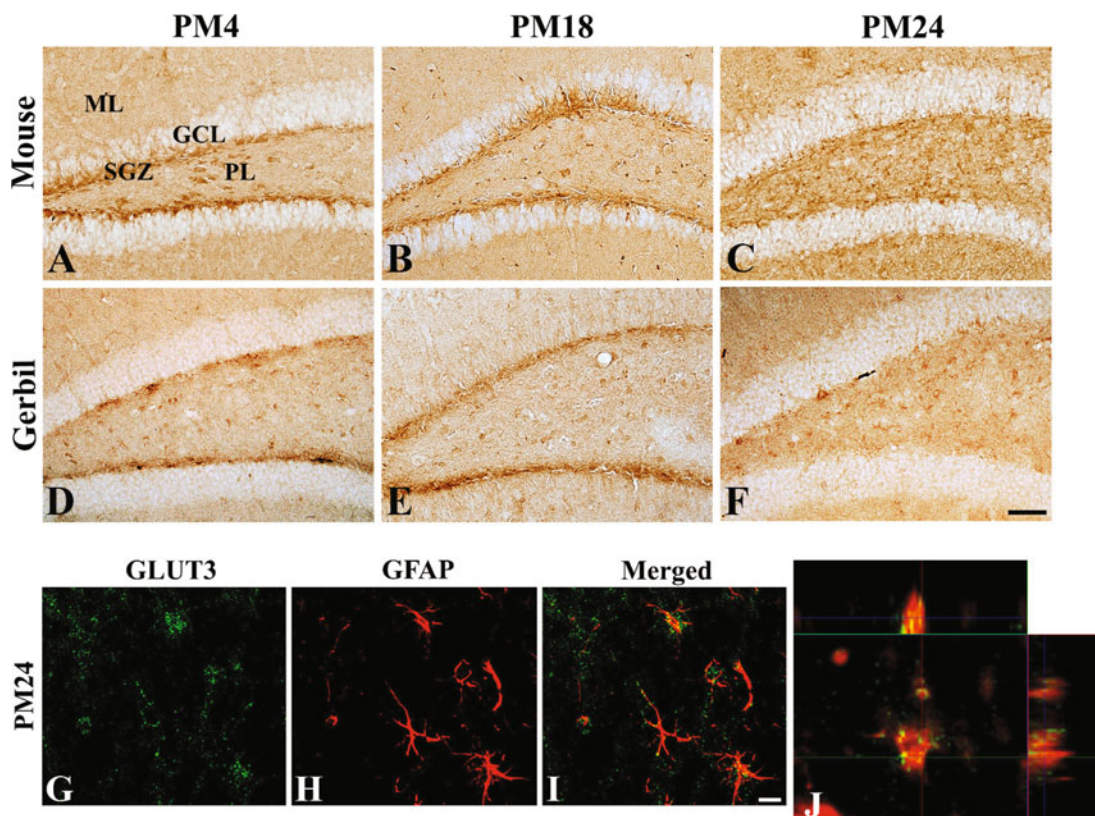

Figure 2. Immunohistochemistry for GLUT3 in the dentate gyrus of mice (A, B, and C) and gerbils (D, E, and F) at postnatal month 4 (PM4, A and D), PM18 (B and E), and PM24 (C and F). In the mice and gerbils at PM4, GLUT3 immunoreactivity is mainly observed in the subgranular zone of the dentate gyrus. GLUT3 immunoreactive structures are less abundant in the dentate gyrus at PM18 and GLUT3 immunoreactivity at PM24 is observed as a dot-like pattern in the PL of dentate gyrus. Scale bar=50 μm. (G-J) Double immunofluorescence staining for GLUT3 (green, G) and GFAP (red, H) (and merged images [yellow, I]) in the dentate gyrus of gerbils at PM24. Note that some of the GLUT3 immunoreactivity is found in the GFAP-immunoreactive astrocytes as shown in magnified orthogonal image (J) at PM24. Scale bar=50 μm. ML, molecular layer; GCL, granule cell layer; PL, polymorphic layer; SGZ, subgranular zone.
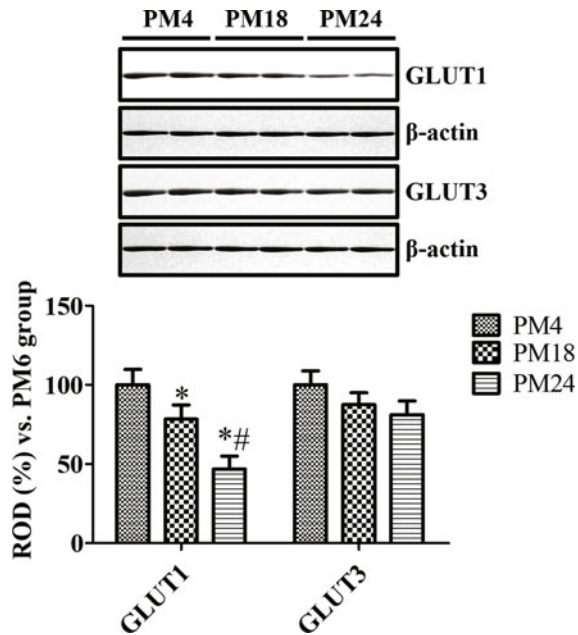
Figure 3. Western blot analysis results are expressed as a percentage of the value of the GLUT1 and GLUT3 immunoblot band in the gerbils at postnatal month 4 (PM4), PM18, and PM24 (*n*=5 per group; *P<0.05, significantly different from the PM4 group; #P<0.05, significantly different from the PM18 group). The values are expressed as mean±SEM.

protein levels in gerbils at PM18 were significantly decreased in the dentate gyrus homogenates compared to that in the gerbils at PM4. In the dentate gyrus of mice and gerbils at PM24, fewer GLUT1 immunoreactive blood vessels were found and GLUT1 protein levels were significantly lower in the gerbils at PM24 and were about 46.8% of the levels in the gerbils at PM4 (Figure 3).

Age-related changes in GLUT3 immunoreactivity and protein levels in the dentate gyrus

In the mice and gerbils at PM4, GLUT3 immunoreactivity was found in the polymorphic layer and subgranular zone of the dentate gyrus although GLLUT3 immunoreactive neurons were abundant in the mice. In the mice and gerbils at PM18, the distribution pattern of GLUT3 immunoreactivity was similar to those in the mice and gerbils at PM4, respectively. In the mice and gerbils at PM24, only a few GLUT3-immunoreactive neurons were detected in the subgranular zone of the dentate gyrus, while GLUT3 immunoreactivity were abundantly observed in the glial components located in the polymorphic layers of the dentate gyrus in mice and gerbils (Figure 2). GLUT3 protein levels in the gerbils were gradually decreased with age in the dentate gyrus

homogenates although statistical significances were not detected (Figure 3).

Colocalization of GLUT3 immunoreactive structures in astrocytes of aged hippocampus

In the aged dentate gyrus of gerbils, GLUT3 immunoreactive structures were mainly found in the polymorphic layer of dentate gyrus. Double immunofluorescence study showed that GLUT3-immunoreactivity was found in the GFAP-immunoreactive astrocytes in the dentate gyrus (Figure 2).

Discussion

During the aging process, the ability to respond to metabolic challenges is progressively reduced and cognitive function impaired by fatigue related to cognitive tasks [23,24] and glucose utilization [11,12]. Comparison of the data for the aged rats at PM27 with that for the adult control rats at PM12 reveals a significant decline (~11%) in glucose uptake [25]. The extracellular glucose was significantly lower in the aged rats and contributed to the age-related deficits in learning and memory [26]. In addition, the administration of glucose transiently enhances the cognitive deficits in aged rats [26].

In the present study, we investigated the two major brain GLUTs involved in transporting the glucose across the blood-brain barrier (GLUT1) and the neurons (GLUT3) in the dentate gyrus of mice and gerbils. GLUT1 immunoreactivity was found in the blood vessels and was significantly decreased in the dentate gyrus of mice and gerbils with age. This result is consistent with previous studies reporting decreased GLUT1 expression in the hippocampus and cerebral cortex of the Alzheimer's disease brain [12,27-29]. With respect to the aging process, there have been conflicting reports regarding the changes in hippocampal GLUT1 expression. Senescence-accelerated mouse resistant 1 (SAMR1), which is a control strain for SAM prone 8 (SAMP8) strain, mice at PM12 show significantly increased GLUT1 expression in both the cortex and the hippocampus compared to SAMR1 mice at PM4 [12]. However, it has been reported that GLUT1 expression in the hippocampus at PM18 was significantly lower (~60% lower) than that at PM8 [30]. In the present study, we observed the significant decreases in GLUT1 expression in the dentate gyrus of mice and gerbils at PM18 compared to those of mice and gerbils at PM4, respectively,

although the expression of GLUT1 further decreased in the dentate gyrus of gerbils and rats at PM24. This result suggests that the glucose in the blood may not be supplied to the brain sufficiently via the blood-brain barrier in the mice and gerbils from PM18.

In this study, we also investigated age-related changes in cell-specific GLUT3 expression in the dentate gyrus of mice and gerbils. In adult dentate gyrus, GLUT3 expression was mainly found in the subgranular zone of the dentate gyrus. In the previous study, our colleagues showed that GLUT3 is expressed in DCX-immuno-reactive neuroblasts during postnatal development in the mouse dentate gyrus [18] and in normal and ischemic gerbil dentate gyrus [31]. GLUT3 expression can be activated by the binding between the promoter region and the phosphorylated cyclic AMP-regulatory element-binding (pCREB) protein and the mouse Y box-binding protein-1 [32]. In addition, the pCREB protein may induce the expression of brain-derived neurotrophic factor, which increases neurogenesis in the hippocampus [33,34]. In our study, we could not find any statistical significances on the GLUT3 expression between PM4 and PM18 groups although GLUT3 immunoreactivity and protein levels were slightly decreased in the dentate gyrus homogenates at PM18 group. This result suggests that GLUT3 is more resistant to age-related changes compared to that in the GLUT1. In the present study, few GLUT3-immunoreactive cells were found in the subgranular zone of the dentate gyrus in mice and gerbils at PM24. However, GLUT3 immunoreactivity was abundantly found in the glial components located in the polymorphic and inner molecular layers of the dentate gyrus. This difference may be associated with the sustained levels of GLUT3 expression by western blot analysis. In the present study, we observed that GLUT3-immunoreactive dot-like structures were expressed in the GFAP-immunoreactive astrocytes in the dentate gyrus of gerbils at PM24. A previous study showing that GLUT3 expression is significantly lower in both the cortex and hippocampus of aged SAMR1 mice compared to that in adult SAMR1 mice [12]. In a mouse model for Alzheimer's disease, SAMP8, the GLUT3 immuno-reactivity is significantly lower at PM12 compared to that observed in age-matched SAMR1 mice [12]. In addition, hippocampal homogenates from middle-aged rats at PM12-PM14 show significantly lower GLUT3 expression compared to homogenates derived from adult rats at PM3 [35]. However, other studies have reported that GLUT3 immunoreactivity is significantly lower in the inner molecular layer of the dentate gyrus in aged female Wistar rats at PM28 compared to that in female Wistar rats at PM11 [17]. In the present study, we observed GLUT3 immunoreactive structures were shown in the astrocytes of dentate gyrus. GFAP, not glutamine synthetase or S100β, mRNA and protein levels are significantly increased in the hippocampus of aged mice [36]. Transient glucose deficiency increases astrocyte membrane capacitance and astrocytes rapidly respond to metabolic dysfunctions [37]. In ischemic animals, GLUT3 is expressed in the astrocytes to take up glucose more rapidly and protect neurons from ischemic damage [14,15,31,38].

In conclusion, GLUT1-immunoreactive microvessels in the dentate gyrus and GLUT3-immunoreactive structures in the subgranular zone of dentate gyrus are significantly fewer with age and GLUT3 is expressed in the astrocytes in the group of mice and gerbils at PM24. This result suggests that GLUT1 is more susceptible to age-related changes of glucose transporting systems compared to that in the GLUT3 and the translocation of GLUT3 immunoreactivity from neurons to astrocytes may be associated with the age-related decline in hippocampal function or compensatory mechanisms to respond to metabolic dysfunction.

Acknowledgments

Conflict of interests The authors declare that there is no financial conflict of interests to publish these results.

References

1. Clark DD, Sokoloff L. Circulation and energy metabolism of the brain. In: Basic neurochemistry: molecular, cellular and medical aspects (Siegel GJ, Agranoff BW, Albers RW, Fisher SK, Uhler MD, eds), 6th ed, Lippincott-Raven, Philadelphia, 1999; pp. 637-670.
2. Flier JS, Mueckler M, McCall AL, Lodish HF. Distribution of glucose transporter messenger RNA transcripts in tissues of rat

and man. J Clin Invest 1987; 79(2): 657-661.

3. Yano H, Seino Y, Inagaki N, Hinokio Y, Yamamoto T, Yasuda K, Masuda K, Someya Y, Imura H. Tissue distribution and species difference of the brain type glucose transporter (GLUT3). Biochem Biophys Res Commun 1991; 174(2): 470-477.

4. Nagamatsu S, Kornhauser JM, Burant CF, Seino S, Mayo KE, Bell GI. Glucose transporter expression in brain. cDNA sequence of mouse GLUT3, the brain facilitative glucose transporter isoform, and identification of sites of expression by in situ hybridization. J Biol Chem 1992; 267(1): 467-472.

5. Gerhart DZ, LeVasseur RJ, Broderius MA, Drewes LR. Glucose transporter localization in brain using light and electron immunocytochemistry. J Neurosci Res 1989; 22(4): 464-472.

6. Pardridge WM, Boado RJ, Farrell CR. Brain-type glucose transporter (GLUT-1) is selectively localized to the blood-brain barrier. Studies with quantitative western blotting and in situ hybridization. J Biol Chem 1990; 265(29): 18035-18040.

7. Dick AP, Harik SI, Klip A, Walker DM. Identification and characterization of the glucose transporter of the blood-brain barrier by cytochalasin B binding and immunological reactivity. Proc Natl Acad Sci USA 1984; 81(22): 7233-7237.

8. Heilig CW, Saunders T, Brosius FC 3rd, Moley K, Heilig K, Baggs R, Guo L, Conner D. Glucose transporter-1-deficient mice exhibit impaired development and deformities that are similar to diabetic embryopathy. Proc Natl Acad Sci USA 2003; 100(26): 15613-15618.

9. Jensen PJ, Gitlin JD, Carayannopoulos MO. GLUT1 deficiency links nutrient availability and apoptosis during embryonic development. J Biol Chem 2006; 281(19): 13382-13387.

10. Zhao Y, Fung C, Shin D, Shin BC, Thamotharan S, Sankar R, Ehninger D, Silva A, Devaskar SU. Neuronal glucose transporter isoform 3 deficient mice demonstrate features of autism spectrum disorders. Mol Psychiatry 2010; 15(3): 286-299.

11. Willis MW, Ketter TA, Kimbrell TA, George MS, Herscovitch P, Danielson AL, Benson BE, Post RM. Age, sex and laterality effects on cerebral glucose metabolism in healthy adults. Psychiatry Res 2002; 114(1): 23-37.

12. Zhang X, Li G, Guo L, Nie K, Jia Y, Zhao L, Yu J. Age-related alteration in cerebral blood flow and energy failure is correlated with cognitive impairment in the senescence-accelerated prone mouse strain 8 (SAMP8). Neurol Sci 2013; 34(11): 1917-1924.

13. Dornbos D 3rd, Zwagerman N, Guo M, Ding JY, Peng C, Esmail F, Sikharam C, Geng X, Guthikonda M, Ding Y. Preischemic exercise reduces brain damage by ameliorating metabolic disorder in ischemia/reperfusion injury. J Neurosci Res 2013; 91(6): 818-827.

14. Iwabuchi S, Kawahara K, Harata NC. Effects of pharmacological inhibition of AMP-activated protein kinase on GLUT3 expression and the development of ischemic tolerance in astrocytes. Neurosci Res 2014; 84: 68-71.

15. Iwabuchi S, Kawahara K. Inducible astrocytic glucose transporter-3 contributes to the enhanced storage of intracellular glycogen during reperfusion after ischemia. Neurochem Int 2011; 59(2): 319-325.

16. Choeiri C, Staines W, Messier C. Immunohistochemical localization and quantification of glucose transporters in the mouse brain. Neuroscience 2002; 111(1): 19-34.

17. Fattoretti P, Bertoni-Freddari C, Casoli T, Di Stefano G, Solazzi M, Giorgetti B. Decreased expression of glucose transport protein (Glut3) in aging and vitamin E deficiency. Ann N Y Acad Sci 2002; 973: 293-296.

18. Jung HY, Yim HS, Yoo DY, Kim JW, Chung JY, Seong JK, Yoon YS, Kim DW, Hwang IK. Postnatal changes in glucose transporter 3 expression in the dentate gyrus of the C57BL/6 mouse model. Lab Anim Res 2016; 32(1): 1-7.

19. Fox JG, Barthold SW, Davisson MT, Newcomer CE, Quimby FW, Smith AL. The Mouse in Biomedical Research: Normative Biology, Husbandry, and Models, 2nd ed, American College of Laboratory Animal Medicine (Elsevier), Burlington, 2007; pp 1-

759.

20. Franklin KBJ, Paxinos G. The Mouse Brain in Stereotaxic Coordinates. Academic Press, San Diego, 1997; pp 1-190.

21. Loskota WJ, Lomax P, Verity MA. A Stereotaxic Atlas of the Mongolian Gerbil Brain (*Meriones unguiculatus*). Ann Arbor Science, Ann Arbor, 1974; pp 1-157.

22. Hahn KR, Jung HY, Yoo DY, Kim JW, Kim YH, Jo YK, Kim GA, Chung JY, Choi JH, Hwang IK, Jang G, Yoon YS. Immunohistochemical localization of glucose transporter 1 and 3 in the scrotal and abdominal testes of a dog. Lab Anim Res 2017; 33(2): 114-118.

23. Deary IJ, Sommerfield AJ, McAulay V, Frier BM. Moderate hypoglycaemia obliterates working memory in humans with and without insulin treated diabetes. J Neurol Neurosurg Psychiatry 2003; 74(2): 278-279.

24. McNay EC. The impact of recurrent hypoglycemia on cognitive function in aging. Neurobiol Aging 2005; 26 Suppl 1:76-79.

25. Meier-Ruge W, Kolbe M, Sattler J. Investigations of the cholinergic deficit hypothesis in the hippocampus of the aged rat brain with physostigmine and scopolamine. Arch Gerontol Geriatr 1991; 12(2-3): 239-251.

26. McNay EC, Gold PE. Age-related differences in hippocampal extracellular fluid glucose concentration during behavioral testing and following systemic glucose administration. J Gerontol A Biol Sci Med Sci 2001; 56(2): B66-B71.

27. Horwood N, Davies DC. Immunolabelling of hippocampal microvessel glucose transporter protein is reduced in Alzheimer's disease. Virchows Arch 1994; 425(1): 69-72.

28. Kalaria RN, Harik SI. Reduced glucose transporter at the blood-brain barrier and in cerebral cortex in Alzheimer disease. J Neurochem 1989; 53(4): 1083-1088.

29. Simpson IA, Chundu KR, Davies-Hill T, Honer WG, Davies P. Decreased concentrations of GLUT1 and GLUT3 glucose transporters in the brains of patients with Alzheimer's disease. Ann Neurol 1994; 35(5): 546-551.

30. Hooijmans CR, Graven C, Dederen PJ, Tanila H, van Groen T, Kiliaan AJ. Amyloid beta deposition is related to decreased glucose transporter-1 levels and hippocampal atrophy in brains of aged APP/PS1 mice. Brain Res 2007; 1181: 93-103.

31. Yoo DY, Lee KY, Park JH, Jung HY, Kim JW, Yoon YS, Won MH, Choi JH, Hwang IK. Glucose metabolism and neurogenesis in the gerbil hippocampus after transient forebrain ischemia. Neural Regen Res 2016; 11(8): 1254-1259.

32. Rajakumar A, Thamotharan S, Raychaudhuri N, Menon RK, Devaskar SU. Trans-activators regulating neuronal glucose transporter isoform-3 gene expression in mammalian neurons. J Biol Chem 2004; 279(25): 26768-26779.

33. Thoenen H. Neurotrophins and neuronal plasticity. Science 1995; 270(5236): 593-598.

34. Finkbeiner S, Tavazoie SF, Maloratsky A, Jacobs KM, Harris KM, Greenberg ME. CREB: a major mediator of neuronal neurotrophin responses. Neuron 1997; 19(5): 1031-1047.

35. Wang BW, Hok V, Della-Chiesa A, Callaghan C, Barlow S, Tsanov M, Bechara R, Irving E, Virley DJ, Upton N, O'Mara SM. Rosiglitazone enhances learning, place cell activity, and synaptic plasticity in middle-aged rats. Neurobiol Aging 2012; 33(4): 835.e13-835.e30.

36. Wu Y, Zhang AQ, Yew DT. Age related changes of various markers of astrocytes in senescence-accelerated mice hippocampus. Neurochem Int 2005; 46(7): 565-574.

37. Lee CY, Dallérac G, Ezan P, Anderova M, Rouach N. Glucose tightly controls morphological and functional properties of astrocytes. Front Aging Neurosci 2016; 8: 82.

38. Yu S, Zhao T, Guo M, Fang H, Ma J, Ding A, Wang F, Chan P, Fan M. Hypoxic preconditioning up-regulates glucose transport activity and glucose transporter (GLUT1 and GLUT3) gene expression after acute anoxic exposure in the cultured rat hippocampal neurons and astrocytes. Brain Res 2008; 1211: 22-29.